Research on characteristics of adsorption and stability of electromagnetic bionic sucker

Luo Tianhong[1], Liang Shuang[2,a,*], Fu Qiang[1], Wang Chenglin[1]

[1]The School of Robot Engineering and Mechanical-Electrical Engineering, Chongqing University of Arts and Sciences, Chongqing, China

[2]School of Mechanotronics and Vehicle Engineering, Chongqing Jiaotong University, Chongqing, China

[a]137377539@qq.com

Keywords: Electromagnetic bionic sucker; Contact load; Time-varying stiffness; nonlinear dynamics

Abstract: To improve the universality and safety of the adsorption system in bridge inspection robot, an electromagnetic bionic composite sucker is proposed. In order to explore the influence of contact excitation and time-varying stiffness on the adsorption stability of electromagnetic bionic suction, the coupling relationship between electromagnetic and bionic sucker is derived based on Hertz contact theory and Maxwell theory, and the surface distortion caused by Maxwell force and Van der Waals force is calculated. The nonlinear dynamics model of composite suction system is established considering the contact load, the surface friction factor, Maxwell stress and time-varying stiffness, adsorption air gap and other factors. Two control parameters are selected to analyze the effect of excitation amplitude and frequency on system stability, and the corresponding simulation is completed. The simulation results show that due to the fluctuation of excitation amplitude and frequency in the adsorption process, the system exhibits obvious nonlinear phenomenon, and the stability of adsorption can be improved by controlling the reasonable threshold.

1. Introduction

With the advancement of "The Belt and Road" policy, the maintenance and construction of bridges has developed rapidly. The traditional bridge inspection is conducted by the bridge inspection vehicle with manual detection, which includes with the problems of low efficiency, local traffic congestion and hidden danger. The bridge inspection robot effectively completes the bridge detection by utilizing intelligent equipment instead of traditional mechanical and manual methods, thus shows effect on solving the above problems.

In recent years, scholars have studied on the adsorption characteristics and nonlinear dynamics of crawling robots. Autumn et al.[1-2] studied the constitutive structure of gecko feet, and analyzed the structure, van Edward force and electrostatic force of the bristle, which revealed the mechanism of adsorption and separation of gecko foot sucker. Lee et al.[3] designed a robot based on vacuum sucker, and analyzed the stability of adsorption through the load variation of the prototype. Sintov et al.[4] studied the adsorption mode of rough surface, and adopted a sucker consisting of several mini steel hooks to achieve adsorption. Gui et al.[5] designed a non-contact gap magnetic adsorption, which realized the adsorption and walking of the curved surface and raised the flexibility of movement. Liu et al.[6] designed a bionic wheeled robot of wall climbing, which is provided with the ability to use circular array to climb concrete and brick walls. The robot distributes the load of two wheels through the spine to ensure the stability of the adsorption. Tavakoli et al.[7] proposed a wheeled climbing robot which can walk on the plane and surface, and compensated the error caused by the wheel skidding through temporarily closing the position control loop, so as to ensure the motion accuracy of the robot. Chen et al.[8] confirmed the analysis and prediction through the numerical analysis methods such as phase diagram, Poincare diagram and bifurcation diagram, and

revealed the effect of excitation amplitude and damping on the chaotic transition of permanent magnet synchronous motor system. In the field of gear system[9-13], scholars applied nonlinear dynamic equations to the kinematic characteristics and malfunction analysis of gears.

Scholars have great achievements in research on crawling robots and adsorption, but few studies on the nonlinear dynamic characteristics of electromagnetic biomimetic composite adsorption. The stability of the robot is directly related to the safety and reliability of the detection. In order to provide reference for the selection of the parameters in the design process of the bridge detection robot, it is urgent to study and analyze the stability of the adsorption, and provide reference for the selection of the parameters in the design process of the bridge detection robot. In this paper, a nonlinear dynamic model of the composite adsorption system is established based on molecular contact load and time-varying contact stiffness, and the influence of excitation amplitude and frequency on the adsorption stability is discussed by the analysis of the model.

2. Design of electromagnetism bionic adsorption mechanism

The core content of the bridge inspection is the detection quality and safety. Therefore, when the detection targets turn to the bottom or pier of the bridge, the adsorption force provided by the adsorption system should ensure that the robot can fulfil photograph steadily during the detection, and avoids to acute vibration or overturning. The difference of the shape of the bridges vary. The bridge deck not only exists the horizontal and vertical surface, but also the arch bridge with the arc. Therefore, the suction system should be able to complete the stable adsorption on the different types of surface and cooperate with the leg mechanism to complete a series of bridge detection work.

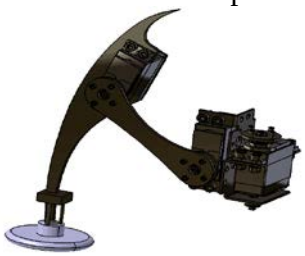

Fig 1. The structure of the leg and sucker of a robot

Electromagnetic suction cups are flexible to achieve adsorption or desorption, but such electromagnetic sucker with high power ratio are often expensive and fail to be applied in large quantities limited to domestic technology. In addition, the adsorption capacity of electromagnetic sucker is often greatly reduced for less rigid material. The biomimetic sucker, based on the imitation of the house lizard ciliary structure, uses Van der Waals force to achieve adsorption without additional adsorption energy, but the threshold of the adsorption force is difficult to control when the surface roughness of the adsorbent is changed.The increase of adsorption force gives rise to the difficulty of the desorption, and hinders the efficiency of the robot. The decrease of the adsorption force reduces the safety of robot in operation, and even sets the robot in the risk of falling. Based on the above characteristics, the electromagnetic bionic sucker is proposed in this paper. As shown in Figure 1, the suction disc is composed of the upper end electromagnetic sucker and the lower end bionic sucker. The electromagnetic sucker is connected to the foot of the robot, and the surface of the bionic suction disc is in contact with the bridge surface to complete the adsorption. The biomimetic sucker underneath has the ciliated structure of imitation house lizard, which uses the characteristics of biomimetic materials to provide the basic adsorption force. By controlling the current, the electromagnetic sucker can change the intensity of the electromagnetic force to meet the adsorbability demand of the robot which helps to complete the adsorption and desorption of the foot.

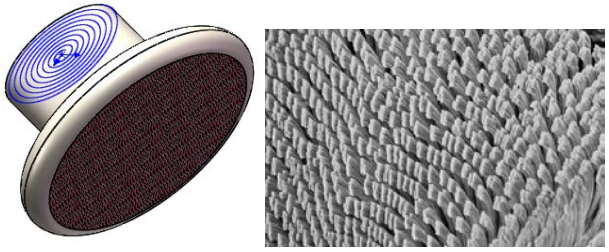

a.Suction cup b. Partial drawing of the bottom

Fig 2. The structure of a bionic sucker

3. Analysis of surface adsorption on unstructured environment

3.1 The Mechanism of Intermolecular Force Excitation

According to the Hertz Theory [11], the elastic contact between the particles on the suction cup and the wall is related to the size of the repulsive energy. Therefore, the Van der Waals potential and the Van der Waals force between the contact molecules conform to the Lennard-Jones formula.

$$U_v = \frac{N}{z^{12}} - \frac{C}{r^6} = 4U_0[(\frac{a}{z})^{12} - (\frac{a}{z})^6] \tag{1}$$

$$F_v = -\frac{dU}{dz} = \frac{12N}{z^{13}} - \frac{6C}{z^7} \tag{2}$$

Where a, z mean molecular radius and spacing, respectively, U_0 is the action potential and define initial action potential $U_0 = -U_{\min} = C/(2z_0^6)$, z_0 is the equilibrium spacing and its value is about $z_0 = (2N/C)^{1/6} = 2^{1/6}a = 1.12a$,C is the London coefficient, and its value is about $10^{-79} J \cdot m^6$;when $z = (13/7)^{1/6} z_0 \approx 1.109 z_0$,Maximum force $F_{\max} = -2.69U_0 / z_0$.

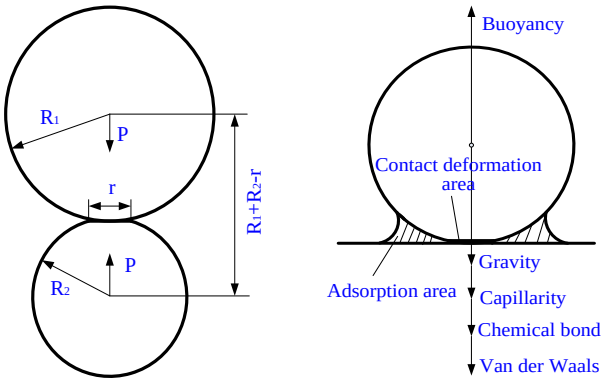

Fig 3. Mechanical model of molecular adhesion

Besides, K is deformation coefficient, w is adhesion work,and $w = \sqrt{\gamma_1 \gamma_2}$, γ_1, γ_2 are surface energy of contact particles, respectively, r_0 is the deformation radius of the particles during contact period, the relation between its value and the external force of the particle is:

$$r_0^3 = \frac{R_i}{K}(F + 3\pi w R_i + \sqrt{6\pi w R_i + (3\pi w R_i)^2}) \tag{3}$$

Stress in the contact area $p(r)$ can be expressed:

$$p(r) = p_0\sqrt{1 - r^2/r_0^2} - \frac{p_0^{'}}{\sqrt{1 - r^2/r_0^2}} \tag{4}$$

Where $p_0 = 3r_0 K / 2\pi R$, $p_0^{'} = \sqrt{3wK/2\pi r_0}$ and $q_0 = p_0^{'}/p_0$ The attraction force F_y and repulsion force F_c can be obtained by integrating the contact area distribution.Thus the resultant force of inter molecular

force $F_s = F_y + F_c$ is obtained:

$$F_y = \int_{r_c}^{r_0} 2\pi p(r) r dr = -\frac{4}{3} q_0^{3/2} \pi r_0^2 p_0 \tag{5}$$

$$F_c = \int_0^{r_0} 2\pi p(r) r dr = (\frac{2}{3} - 2q_0)\pi r_0^2 p_0 \tag{6}$$

$$F_s = F_y + F_c \tag{7}$$

3.2 Electromagnetic force excitation analysis

The electromagnetic adsorption is used as an auxiliary mechanism to protect the robot's stability by combining with the Van der Waals force of biomimetic adsorption. The basic principle of electromagnetic adsorption is based on the electromagnetic force produced by the electric coil. Main parameters include the capacitance, resistance and inductance of the connecting line, the resistance and inductance of the coil part, the resistance and inductance of the execute part. The equation of the closed loop are:

$$\vec{U}_c = (R_c + R_0)\vec{I}_c + L_0 \frac{d\vec{I}_c}{dt} + \left(L_c \frac{d\vec{I}_c}{dt} + M \frac{d\vec{I}_w}{dt} \right) \tag{8}$$

$$\vec{U}_c = \vec{U}_0 - \frac{1}{C_0} \int_0^t \vec{I}_c dt \tag{9}$$

$$R_w \vec{I}_w + L_w \frac{d\vec{I}_w}{dt} + M \frac{d\vec{I}_c}{dt} = 0 \tag{10}$$

Where $\vec{I}_c$ is the current value in the coil, $\vec{I}_w$ is the current value in the execute part of the coil, M is the magnetization of the medium. When the electric field and magnetic field synchronously change, the first order coupled differential equations related to the vector field are:

$$\nabla \cdot B = 0 \,, \nabla \cdot D = \rho_v \tag{11}$$

$$\nabla \times E = -\frac{\partial B}{\partial t} - J_m \,, \nabla \times H = J_e + \frac{\partial D}{\partial t} \tag{12}$$

At this time, there is magnetizing current I_v inside the suction cup, and is magnetized current I_s in the surface, whose current density are δ_v and δ_s respectively .

$$\delta_v = \nabla \times M \qquad (13), \delta_S = -\vec{n} \times M \tag{13}$$

Where $\vec{n}$ is the normal vector of the suction plate surface. Therefore, the adsorption force between the electromagnetic sucker and the magnetic conductive material is:

$$\begin{aligned} F_e &= \iiint_V \delta_v \times B dV + \oiint_S \delta_s \times B dS \\ &= \iiint_V (\nabla \times M) \times B dV + \oiint_S (-\vec{n} \times M) \times B dS \end{aligned} \tag{14}$$

When sucker and magnetic conducting material achieve near vacuum adsorption and air gap adsorption,

$$F_e = \iiint_V (\nabla \times M) \times B dV = \frac{\mu_r - 1}{2\mu_0 \mu_r} \iint_s B^2 ds \tag{15}$$

4. Variable stiffness nonlinear dynamic equation

It is assumed that m_1 and m_2 are the mass of the bionic sucker and the electromagnetic sucker in the system, and c_1 and c_2 are the damping of the bionic the electromagnetic sucker in the system respectively, and k_1 and k_2 are the initial stiffness of the bionic and the electromagnetic sucker in the system. The kinetic energy of the system T is composed of the translational kinetic energy of the centroid of the electromagnetic sucker and the elastic energy of the elastic imitating sucker.

$$T = \frac{1}{2}m_1\dot{x}_1^2 + \frac{1}{2}m_2\dot{x}_2^2 \tag{16}$$

The potential energy of the system is the potential energy of a bionic suction cup.

$$U = \frac{1}{2}k_1 x_1^{\ 2} + \frac{1}{2}k_2 x_2^{\ 2} \tag{17}$$

Lagrange dynamic equation of system can be expressed:

$$\frac{d}{dt}\frac{\partial T}{\partial \dot{\theta}_i} - \frac{\partial T}{\partial \theta_i} + \frac{\partial U}{\partial \theta_i} = Q_i \tag{18}$$

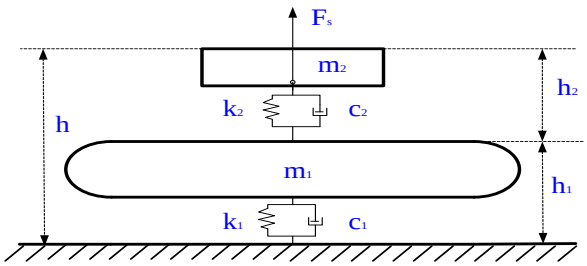

Fig 4. Mechanical model of suction plate adsorption

In the form of generalized force, in this paper:

$$Q = -(c_1\dot{x}_1 + c_2\dot{x}_2) + F_s + \overline{F}_v \tag{19}$$

k is the time varying stiffness, the expression is as follows:

$$k = k_0 + \frac{\xi}{2}(c_1 + c_2) \tag{20}$$

where $k_0 = 2 + 0.03 f_m$, ξ is the conversion coefficient, f_m is the basis friction factor. In addition, the displacement function is $f(x) = \eta_1 x^3 + \eta_2 x^2 + e(x)$,where $e(x)$ is vibration error,which can be ignored in this article, η_1, η_2 is displacement coefficient. Therefore, the kinetic model of adsorption is as follow:

$$m_e\ddot{x} + (c_1 + c_2)\dot{x} + k(t)f(x) = F_s + \overline{F}_v \tag{21}$$

The normalization of the upper form is obtained.

$$\omega_n = (\frac{k}{m_e})^{1/2};\ \bar{t} = \omega_n t;\ \xi = \frac{c_1 + c_2}{2m_e\omega_n};\ \Omega = \frac{\omega_1}{\omega_n};\ \mu = \frac{2\xi}{m\Omega};\ \beta = \frac{k\eta_2}{m\Omega^2};\ \gamma = \frac{k\eta_1}{m\Omega^2};\ F_s = \frac{\overline{F}_s}{m_e h_1 \omega_n^2};\ F_v(\bar{t}) = \frac{\overline{F}_v}{m_e h_1 \omega_n} = F_{vt}\cos\Omega\bar{t};$$
$$f\cos\omega t = F_{vt}\cos\Omega t$$

The dynamic model can also be written:

$$m_e\ddot{x} + 2\xi\dot{x} + k(t)f(x) = F_s + F_{vt}\cos\Omega t \tag{22}$$

Using the time scale $\tau = \Omega t$,The differential equation can be changed into:

$$\ddot{x} + \mu\dot{x} + kx + \beta x^2 + \gamma x^3 = F_s + f\cos\omega t \tag{23}$$

5. Numerical simulation analysis

In order to facilitate numerical simulation, the dynamic model can be written as follows:

$$\begin{cases} \dot{x} = y \\ \dot{y} = F_s + f\cos\tau - \mu\dot{x} - kx - \beta x^2 - \gamma x^3 \end{cases} \tag{24}$$

A series of numerical simulations has been performed using the four-order Runge-kutta method to obtain some information of chaotic behavior of system.

TABLE I. Main parameters of adsorption mechanism

Parameter	Value	Unit
Height of bionic sucker h_1	30	mm
Capacitance C_0	35	μF
Friction coefficient f_m	0.1	
Equivalent mass coefficient c_e	5.04	
Mass of bionic sucker m_1	0.1	kg
Damping of bionic sucker c_1	0.8	Ns/m
Displacement coefficient η_1	0.1	
Height of ele-mag sucker h_2	30	mm
Resistance R_0	25	Ω
Inductance L_0	75	mH
Magnetization intensity M	220	emu/g
Mass of ele-mag sucker m_2	0.2	kg
Damping of ele-mag sucker c_2	10	Ns/m

we choose f as control parameter to analyze the impact of its changes on the system. Figure 5 is a bifurcation diagram of a dimensionless value x using f as control parameter ($\mu = 1.2$, $k = 1$, $\beta = 0.85$, $\gamma = 0.2$, $\omega = 1$)..

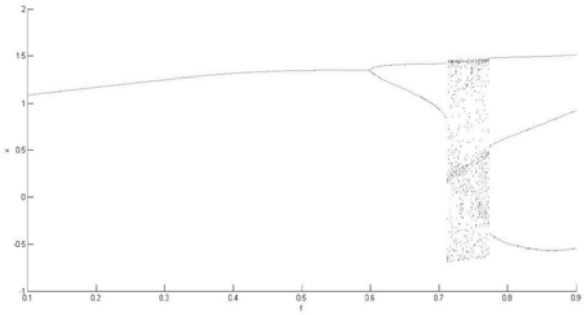

Fig 5. Bifurcation diagram using f as control parameter

By observing the bifurcation diagram with excitation amplitude f as control parameter, we can intuitively deduce that there are rich motion states in the system. When $f \le 0.595$, the system has been presented as a 1T-periodic motion, but as the value increases to the 0.595, the 1T-periodic motion converts to a 2T-period, while the system is still in a stable state. With the further increased, the system jumps into chaotic state after period doubling bifurcations.Finally, the system presents a 3T-periodic motion from the degenerate doubling bifurcation of chaotic motion and return to steady state.

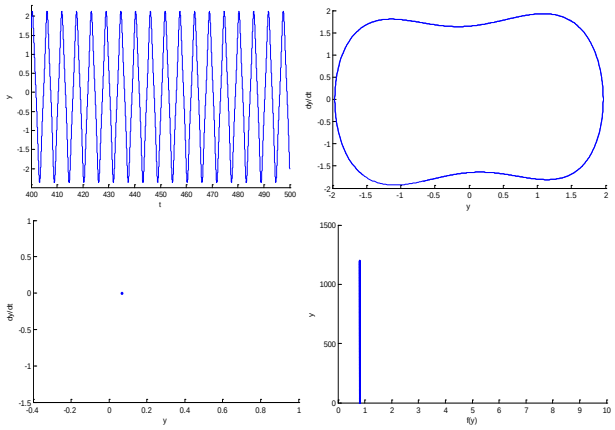

a. $f = 0.4$

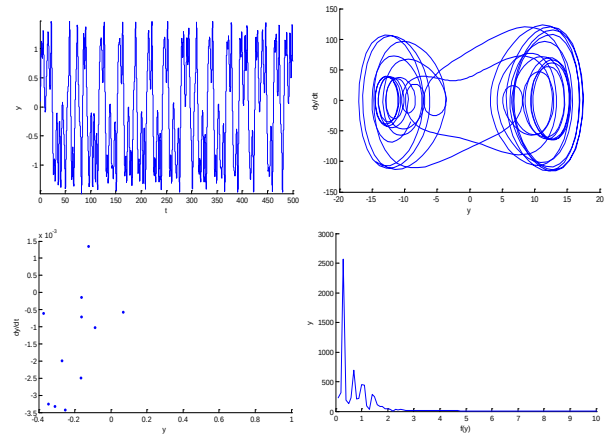

b. $f = 0.75$

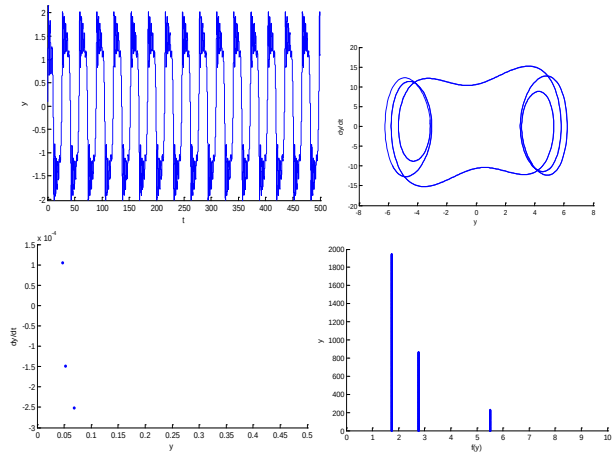

c. $f = 0.85$

Fig 6. Phase diagram, time history, Poincare cross section and amplitude frequency diagram with variability f

To further explain the influence of the excitation frequency f on the dynamic behavior of the system, the phase diagram, the time history, the Poincare map and the amplitude frequency diagram of the three different motion states($f = 0.4$, $f = 0.75$, $f = 0.85$) are analyzed and explained respectively. From Fig.6, we can see that when the excitation frequency changes, the system experiences periodic and chaotic motion states. When $f = 0.4$, the time history is a single peak periodic motion of the rule, and the phase diagram shows one closed circle, while the Poincare map is an isolated point. and the amplitude spectrum was shown as an isolated peak, which associates with the characteristic of one discrete strip in the periodic motion . As the control parameter f is further increased, it can be found that the motion of the system was no longer in a stable state and

transformed into a chaotic motion. In the time history, the peaks are varied and irregular, and there are many irregular closed rings in the phase diagram, and the amplitude spectrum is shown as a continuous line, which accords with the characteristics of chaotic motion.

With the further change of the excitation frequency, the system of chaotic motion degenerate the doubling bifurcation into the 3T-periodic motion. The time history is the regular periodic motion, and the phase diagram shows three closed rings. The Poincare map is several points, and the frequency spectrum is shown as three isolated peaks, which conforms to the periodic motion.

6. Conclusion

The parameters such as contact friction and excitation play a decisive role in the stability of the electromagnetic bionic sucker. Based on the Hertz contact theory and Maxwell theory, the coupling mechanism of the bionic force and electromagnetic force is explored, and the changing laws of the excitation are obtained. On this basis, the nonlinear dynamics model of the adsorption system are established. Some conclusions are as follows:

(1) Through numerical simulation, it is found that with the increase of the control parameter f, the system has experienced three processes of the 1T-periodic motion, the 2T-periodic motion and the chaotic motion. The above phenomena indicate that in the design of suction cups, the external excitation of high frequency and high amplitude should be avoided to meet stability requirement in the process of robot adsorption in the situation of the minimum adsorption force.

(2) There is a rich nonlinear dynamic phenomenon in the electromagnetic bionic composite adsorption system. By controlling the parameters of different values, the system has a stable motion of periodic motion and instability. According to the simulation results, the selection of the parameters of the sucker system can effectively improve the stability of the system, and provide some theoretical guidance for the design and application of the robot.

References

[1] K Autumn, Y A Liang, S Hsieh,. Adhesive force of a single gecko foot-hair. Nature, 2000, pp: 405:681.

[2] K Autumn, M Sitti, Y A Liang,. Evidence for van der Waals adhesion in gecko setae. Proceedings of the Nati Aca of Sciences of the USA, vol.99, 2002, pp: 12252.

[3] G Lee, H Kim, K Seo. MultiTrack: A multi-linked track robot with suction adhesion for climbing and transition. Rob & Auto Systems, vol.72, 2015, pp:207.

[4] A Sintov, T Avramovich, A Shapiro. Design and motion planning of an auto climbing robot with claws. Rob & Auto Systems, vol.59, 2011,pp:1008.

[5] Z Gui, Q Chen, Z Sun. Wall climbing robot employing multi-body permanent magnetic adhesion system. Chinese Journal of Mechanical Engineering,vol44,2008,pp:177.

[6] Y Liu, S Sun, X Wu,. A Wheeled Wall-Climbing Robot with Bio-Inspired Spine Mechanisms. Journal of Bionic Engineering, vol.12,2015,pp:17.

[7] M Tavakoli, P Lopes, L Sgrigna,. Motion control of an omnidirectional climbing robot based on dead reckoning method. Mechatronics, vol.30, 2015,pp.94.

[8] X Chen, J Hu, Z Peng,. Bifurcation and chaos analysis of torsional vibration in a PMSM-based driven system considering electromechanically coupled effect[J]. Nonlinear Dynamics, vol1,2017.

[9] G Zhang, Q Yin, D Jiang. Research on Nonlinear Dynamics of Five-DOF Active Magnetic Bearings-rotor System. Chinese Journal of Mechanical Engineering, vol.46,pp.15,2010.

[10] R Ma, Y Chen. Nonlinear Dynamic Research on Gear System with Cracked Failure. Chinese Journal of Mechanical Engineering, vol.47,pp. 84,2011.

[11] T Sun, Y Shen, Z Sun. Study on nonlinear dynamic behavior of planetary gear train solution and dynamic behavior analysis. Chinese Journal of Mechanical Engineering, vol38,pp.11,2002.

[12] X Gou, C Qi, D Chen. Nonlinear Dynamic Modelling and Analysis of Gear System with Tooth Contact Temperature. Chinese Journal of Mechanical Engineering, vol.51,pp. 71,2015.

[13] G Li, G Yu, J Wen Method of multiple scales in solving nonlinear dynamic differential equations of gear systems. Journal of Jilin University, vol.38, pp.75, 2008.

[14] Q Huang, Q Wang. Analysis of time-variant stiffness excitation effects of elastoplastic dynamic structural systems. China Civil Engneeiring Journal, vol.39.